

Rosby Wave Breaking in the Southern Hemisphere Wintertime Upper Troposphere

DIETER PETERS

Leibniz-Institut für Atmosphärenphysik, e.V. an der Universität Rostock, Kühlungsborn, Mecklenburg-Vorpommern, Germany

DARRYN W. WAUGH

Department of Earth and Planetary Sciences, The Johns Hopkins University, Baltimore, Maryland

(Manuscript received 9 December 2002, in final form 10 March 2003)

ABSTRACT

The characteristics of Rossby wave propagation and breaking in the Southern Hemisphere upper troposphere during winter are examined. Although the Southern Hemisphere subtropical jet is more zonally symmetric than that of the Northern Hemisphere, there are still significant zonal variations in the upper-tropospheric flow. In particular, the flow within a given sector ($\approx 120^\circ$ longitude) can generally be characterized into one of four different configurations: (i) a single jet, (ii) a “broken” subtropical jet, (iii) a polar jet at the upstream end of the subtropical jet, or (iv) a polar jet at the downstream end of the subtropical jet. Using “potential vorticity thinking” and barotropic wind shear arguments, it is argued that the characteristics of the Rossby wave propagation and breaking will differ between each flow configuration. Consistent with these arguments, examination of potential vorticity maps and contour advection calculations show differing wave-breaking characteristics. In particular, there is “equatorward” wave breaking with cyclonic behavior when a single strong jet exists, “poleward” breaking with anticyclonic behavior when a broken subtropical jet or a polar jet is downstream of a subtropical jet, and more “symmetric” wave breaking when a polar jet is upstream of a subtropical jet. Some of the flow configurations have preferred geographical locations, and this results in different geographical sectors having differing preferred configurations and variability, and, hence, characteristics of the Rossby wave propagation. For example, a broken subtropical jet or polar jet with poleward wave breaking is most common within the Australian and Pacific Ocean sectors.

1. Introduction

Synoptic-scale Rossby waves play an important role in balancing the torque and heat between subtropical and polar regions in the troposphere and lower stratosphere. The propagation of Rossby waves is responsible for links between different locations (“teleconnections”), and the interaction between these transient waves with a period of 2–6 days and the quasi-stationary wind field is a well-known process in determining the position of storm tracks and regions of background wind accelerations (e.g., Hoskins et al. 1983; Trenberth 1991). Furthermore, Rossby waves can produce large scale meridional movement of air, and irreversible horizontal transport between extratropics and subtropics occurs during Rossby wave “breaking” events (McIntyre and Palmer 1983). This Rossby wave breaking in the upper troposphere/lower stratosphere contributes to stratosphere–troposphere exchange and the formation of cut-off cyclones, anticyclones, and blocking events. It is

therefore important to understand the propagation and breaking of Rossby waves in the upper troposphere.

Several previous studies have shown that the latitudinal and longitudinal variations in the basic flow structure strongly influence the characteristics of Rossby wave propagation and breaking. Nakamura and Plumb (1994) examined the importance of the across-jet shear on the direction of the breaking (i.e., the direction of transport of air across the jet), while Nakamura (1994) and Swanson et al. (1997) examined the impact of along-flow variations in jet strength on the location of the wave breaking. The effect of the barotropic deformation field on characteristics of Rossby wave breaking has been discussed by Thorncroft et al. (1993) for “equatorward” events and by Peters and Waugh (1996) for “poleward” events.

The above studies have primarily considered the flow in the Northern Hemisphere (NH), and little attention has been paid to the wave breaking in the Southern Hemisphere (SH). However, as the wintertime large-scale structure of upper-tropospheric flow in the SH differs from that in the NH (e.g., Hoskins et al. 1989; Randel 1992), it is possible that the characteristics of the Rossby-wave-breaking process could differ between

Corresponding author address: Dr. Dieter Peters, Leibniz-Institut für Atmosphärenphysik, Schloßstraße 6, D-18225 Kühlungsborn, Mecklenburg-Vorpommern, Germany.
E-mail: peters@iap-kborn.de

hemispheres. For example, there is a polar jet, with a double-jet structure, in some longitudes in the SH that does not have a counterpart in the NH wintertime flow, and wave breaking in these longitudes could differ from that occurring in the NH.

In this paper we examine the characteristics of Rossby wave breaking in the SH wintertime upper troposphere. The wintertime zonal-wind structures are analyzed, and differences in the flow within longitude sectors (of around 120° longitude) are highlighted. Four different idealized configurations for flow in a sector are identified, and the differences in the evolution of Rossby waves in each of these four configurations are examined using simple horizontal shear arguments in a barotropic atmosphere (called “barotropic shear” for short) and analysis of case studies.

In the next section the datasets used and methods of investigation are described. In section 3 we present our analysis of the wintertime upper-tropospheric flow and identify four different configurations for flow in a sector. The propagation and breaking of Rossby waves in these configurations are then examined in section 4. Implications are discussed in section 5, and concluding remarks are given in section 6.

2. Data and methods

We use monthly mean wind fields on pressure surfaces from the National Centers for Environmental Prediction–National Center for Atmospheric Research (NCEP–NCAR) reanalysis (Kalnay et al. 1996) to examine the mean flow structure, as well as interannual and intraseasonal variability, of the upper-tropospheric flow in both hemispheres. The climatological mean wintertime zonal wind (June–August in the SH; December–February in the NH), as well as the monthly variance about this state, are calculated for the period 1980–99. We also examine individual monthly mean zonal-wind fields.

The daily variations in the wintertime SH flow for 1990–93 are then examined using daily operational analyses from the European Centre for Medium-Range Weather Forecasts (ECMWF). NCEP–NCAR reanalyses are used to examine the interannual and intraseasonal variability as we have easy access to these monthly mean fields, while the ECMWF analyses are used to examine the daily variations as they have higher spatial resolution ($1^\circ \times 1^\circ$) than the NCEP–NCAR reanalyses ($2.5^\circ \times 2.5^\circ$).

Because we are interested in the characteristics of Rossby waves, we examine these data on isentropic surfaces (focusing on the 330-K surface). Time-mean (5–30 days) zonal winds are calculated to examine the basic state in which the waves are propagating. The evolution of Rossby waves is examined using maps of Ertel’s (1942) potential vorticity (EPV) on isentropic surfaces, calculated as in Bartels et al. (1998). EPV is extremely useful for examining large-scale dynamical processes

because it is conserved if the flow is frictionless and adiabatic, and it is possible to deduce all other dynamical fields from knowledge of EPV and boundary conditions [under suitable balance conditions; see, e.g., Hoskins et al. (1985, 1987)].

To further highlight the Rossby wave propagation, and to examine finer-scale structures than resolved by the analyses, we also perform contour advection (CA) calculations (Vaugh and Plumb 1994; Norton 1994). In these calculations material contours are initialized as analyzed EPV contours, and analyzed winds on isentropic surfaces are used to advect these contours (6-hourly analyzed winds are used, with a 30-min time step). An adjustable number of nodes is used to resolve each contour, which enables the contours to develop finescale features that are not resolved in the analyzed EPV (e.g., Plumb et al. 1994; Vaugh et al. 1994; Appenzeller et al. 1996; Peters and Vaugh 1996). The winds used for the advection of the contours are analyzed winds, and not the winds predicted from isentropic EPV fields. Hence, diabatic and baroclinic processes are included in the CA calculations.

In the following calculations, the EPV = -2.5 PVU contour (where $1 \text{ PVU} = 1 \times 10^{-6} \text{ K m}^2 \text{ s}^{-1} \text{ kg}^{-1}$), which represents the dynamical tropopause, is used to initialize the CA calculations. There are usually many small “blobs” of EPV = -2.5 PVU in the ECMWF analyses, but we remove these to form the initial contours for the CA calculations (the contour enclosing the largest area is used for the initial contour).

3. Wintertime wind structure

We first examine the mean wintertime flow in the NH and SH upper troposphere. Figure 1 shows the climatological mean (1980–99) wintertime zonal wind at 300 hPa for (a) the NH (December–February) and (b) the SH (June–August), from the NCEP–NCAR reanalyses. [These mean fields agree well with those from the original NCEP analyses (Randel 1992) and ECMWF analyses (Hoskins et al. 1989), and the features discussed below are observed in all three analyses.] Comparing these plots, we see the well-known differences between the wintertime upper-tropospheric zonal-wind structure in the two hemispheres. The NH subtropical jet is stronger, with larger zonal variations in its magnitude. There is a distinct polar jet over the southern Atlantic and Indian Oceans that has no northern counterpart (the North American jet tilts toward the pole but does not overlap with the jet over Africa). The existence of a polar jet in the SH means that there is a double-jet structure in the eastern Indian Ocean where this jet overlaps the subtropical jet.

Although the SH subtropical jet is more zonally symmetric than that in the NH, there are still significant longitudinal variations in the SH. In particular, both the subtropical jet and polar jet have a pronounced localized maximum: the subtropical jet over the Australia–west-

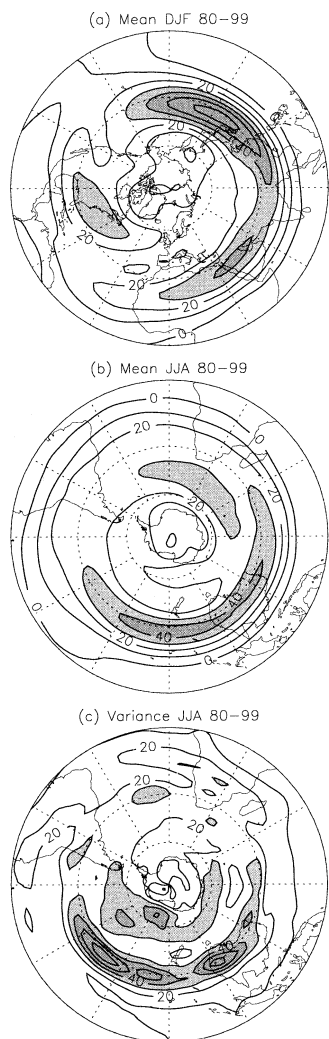


FIG. 1. Maps of 300-hPa zonal wind: (a) climatological mean for NH winter months (Dec–Feb 1980–99), (b) climatological mean for SH winter months (Jun–Aug 1980–99), and (c) monthly standard deviation for SH. Contour interval is 10 m s^{-1} , with values larger than 30 m s^{-1} shaded.

ern Pacific region and the polar jet south of Africa. These variations have important implications for the Rossby wave propagation and breaking.

There is large interannual and intraseasonal variability in both the position and strength of the jets in the SH. This can be seen from Fig. 1c, which shows the variance of the SH monthly mean winds over the 20 winters (60 months). This shows that there are two centers of maximum subtropical-jet variability, one over Australia and the other over the central Pacific Ocean, and one region of high variability of the polar jet north of the Ross Ice Shelf. The variability in the subtropical jet generally involves a zonal movement rather than a latitudinal movement of the jet. In some months the subtropical jet extends across the Pacific to South America (e.g., June–July 1997; not shown), whereas in other

months it ends near the date line (e.g., June–July 1998; not shown). The variability in the polar jet generally corresponds to strengthening of the polar jet over this region, with a strong polar jet occurring in some years (e.g., winter 1989; not shown). These variations in the location or strength of the subtropical jet and polar jet result in large variations in the flow structure in a given geographical sector. This is particularly true for the eastern Indian Ocean–Australia region, where for some periods there are strong subtropical and polar jets (“double”- or “split”-jet structure), while for other periods there is a strong single jet [see Bals-Elsholz et al. (2001) for recent analysis of the variability of the double-jet structure]. In contrast, there is only weak variability over the southern Atlantic, where there is generally a single weak (polar) jet.

Examples of the variability in the monthly mean flow structure in the SH can be seen in Fig. 2, which shows the monthly mean 300-hPa zonal winds for June and July between 1990 and 1993. Consistent with Fig. 1c, the variability is larger over the Indian and Pacific Oceans than over the Atlantic Ocean. The magnitude of the maximum in the monthly mean subtropical jet is similar in all months (around $40\text{--}50 \text{ m s}^{-1}$), but there are large variations in the longitude of this maximum, and in some months there are two maxima. There are also large variations in the strength of the polar jet in the Australia–New Zealand region. Note that the mean meridional wind speed in SH winter months reaches maximum values of only about 10 m s^{-1} , which is relatively weak in comparison to the mean-zonal-wind jets.

As will be discussed in the next section, the zonal and meridional variations of the flow play an important role in the evolution of Rossby waves. Visual inspection of monthly mean plots (as in Fig. 2) for all winter months between 1980 and 1999 shows that there can be large variations in the monthly mean flow structure in a given longitude “sector” (120° longitude), and that there are four characteristic flow configurations that can occur within any sector. An illustration of these four different configurations can be seen by comparing the flow within the $90^\circ\text{--}210^\circ\text{E}$ sector (Australian sector) in the different months shown in Fig. 2. In some months there is a strong subtropical jet throughout the sector, with no polar jet (e.g., July 1990). However, in other months there is a polar jet in this sector, with varying location and strength. In some months between 1980 and 1999 the maximum in the polar jet is south of New Zealand, and the subtropical jet weakens at around the same longitude (e.g., July 1993), while in other months the polar jet is upstream of the maximum in the subtropical jet (e.g., June 1993) or downstream of the subtropical jet maximum (e.g., June 1990).

Schematic diagrams of the four different flow structures mentioned previously are shown in Fig. 3 and can be classified as

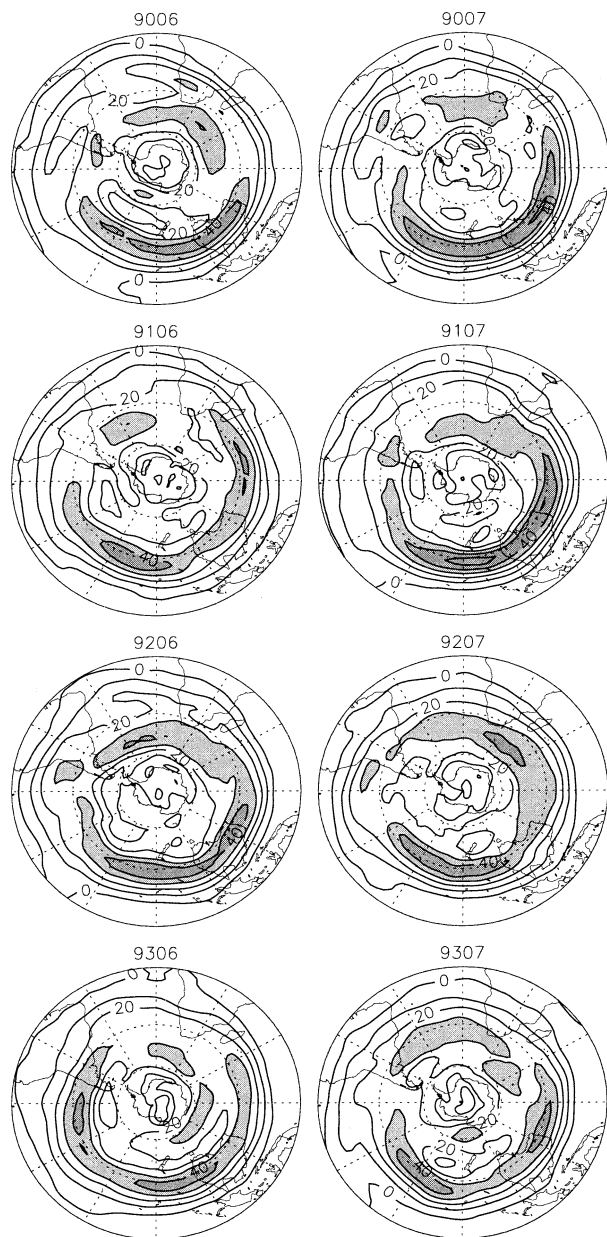


FIG. 2. Maps of monthly mean 300-hPa zonal wind for SH (left) Jun and (right) Jul 1990–93. Contour interval and shading are as in Fig. 1.

- a single jet throughout the sector, referred to as the single-jet (SJ) configuration;
- a break in (weakening of) the subtropical jet within the sector, with a possible strengthening of the polar jet near the longitude of weakening, referred to as the broken-jet (BJ) configuration;
- a polar jet upstream of the subtropical jet, referred to as the double-jet upstream (DU) configuration; and
- a polar jet downstream of the subtropical jet, referred to as the double-jet downstream (DD) configuration.

As expected from the climatological mean location

of the jets (Fig. 1b) and their variability (Fig. 1c), some of configurations have preferred sectors. In particular, the DU configuration occurs most often in the Indian Ocean–Australia region, whereas the DD configuration occurs most often in the New Zealand–Pacific Ocean region. There are two main regions where there is a weakening of the subtropical jet (i.e., the BJ configuration): the Australia–New Zealand region and the eastern Pacific–South America region. The weakening of the subtropical jet over Australia is often accompanied by a strengthening of the polar jet south of New Zealand (e.g., July 1993; Fig. 2). A BJ configuration occurs over the eastern Pacific Ocean when the subtropical jet extends eastward across most of the Pacific and the jet over the Atlantic extends westward and equatorward (e.g., June 1992; Fig. 2).

These preferred regions for different flow configurations mean that different geographical regions have preferred flow configurations. The monthly mean flow in the Indian Ocean sector (0° – 120° E) is generally either in the SJ or DU configuration (with roughly equal occurrence during the 1980–99 period). The flow in the Australian sector (90° – 210° E) is the most variable, and all four configurations occur in this sector. The Pacific Ocean sector (180° – 300° E) is most often in the SJ configuration but, as described above, can be in the BJ configuration. The monthly mean flow in the Atlantic Ocean sector (270° – 30° E) is almost always in the SJ configuration. The above preferred flow configurations refer to the monthly mean flow, but it is important to note that there is submonthly variability and that the flow in a 5–9-day period can differ from the monthly mean flow. For example, Fig. 4 shows a period when there is a double-jet structure over the Atlantic. A further discussion of the submonthly zonal-wind variability is given in section 4b.

The variability in the flow structure discussed above includes both interannual and intraseasonal variability. Numerous studies have examined the variability of the SH flow on both these timescales and shown that the leading mode of variability is zonally symmetric (e.g., Kidson 1988; Nigam 1990; Karoly 1990). The two phases of this mode correspond to a single-jet phase when there is narrow, single jet around 40° S and a double-jet phase when there is a broad, slightly double jet with a maximum around 60° S. In the single-jet phase there is generally a strengthening of the subtropical jet, whereas in the double-jet phase there is a strengthening of the polar jet. Hartmann (1995) argued that there is differing Rossby wave breaking and evolution of cyclones in the latter stages of baroclinic life cycles in the two phases, and that these differences acted to sustain the flow in given flow configuration. However, at the same time, Hartmann (1995) noted that it is unusual for all longitudes to be in the same single- or double-jet configuration; that is, one range of longitudes may be in the opposite phase of the zonal-mean index.

A large portion of the interannual variability is linked

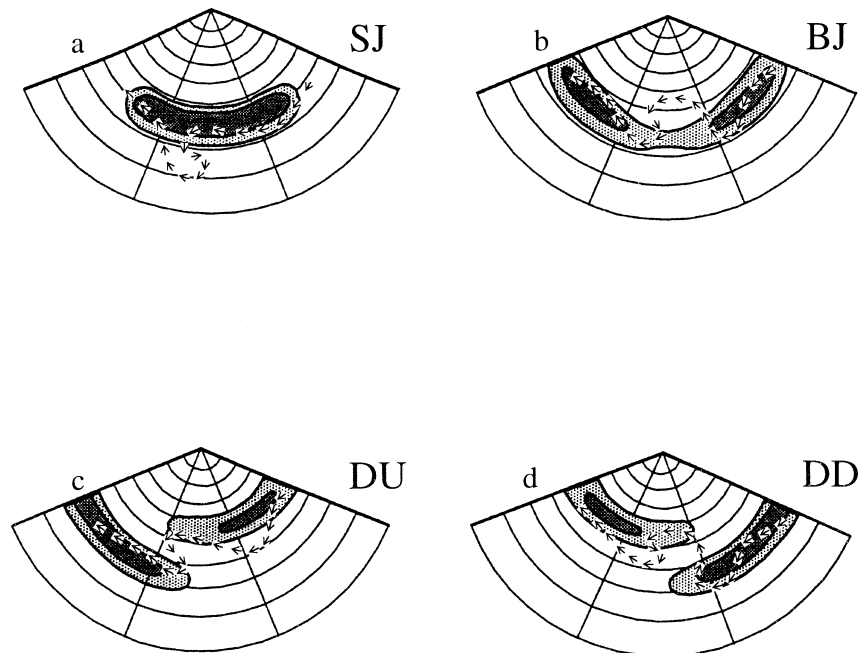


FIG. 3. Schematic diagram of four idealized configurations of zonal wind in a sector: (a) single jet (SJ), (b) broken jet (BJ), (c) double jet upstream of a subtropical jet (DU), and (d) double jet downstream of a subtropical jet (DD). Arrows indicate Rossby wave contour.

with the El Niño–Southern Oscillation (ENSO). There is a stronger subtropical jet and weaker polar jet over the Pacific in the warm phase [minimum Southern Oscillation index (SOI)] and a weaker subtropical jet and stronger polar jet in the cold phase (e.g., Karoly 1989; Chen et al. 1996). However, the variability from month to month within a single ENSO cycle is nearly as large as the variability between different ENSO phases. In fact, the 1990–93 period is within a single (warm) phase of ENSO, and, as can be seen from Fig. 2, there is still large variability in the upper-tropospheric flow within this period.

4. Characteristics of Rossby wave propagation and breaking

As mentioned in the introduction, previous studies have shown that latitudinal and longitudinal variations in the basic flow structure (in particular, the barotropic shear) strongly influence the characteristics of Rossby wave propagation and breaking (e.g., Thorncroft et al. 1993; Nakamura and Plumb 1994; Peters and Waugh 1996). We therefore expect the different flow (shear) structure in the four idealized flow configurations discussed above to result in differing Rossby wave propagation and breaking. Below, we use the “PV thinking” and shear arguments introduced in the above papers to discuss the expected variations, and then we present case studies for periods when the flow in the Australia–central Pacific region was in each of the different configurations. The shear arguments used are linear, but the

above studies have shown that these arguments still provide valuable insight into nonlinear evolution (and the case studies below further confirm this).

For each of the case studies, we use 5-day mean zonal winds to show the basic-state flow (plots of 9-day mean winds are very similar), and maps of the analyzed EPV and CA calculations to show the evolution of Rossby waves. We focus here on the 330-K isentropic surface and use the deformation of the initially smoothed EPV = -2.5 PVU contour, which is representative of the dynamical tropopause.

a. Case studies of Rossby wave breaking

When a sector is in the SJ configuration there is a strong jet throughout the sector, and there are only strong zonal variations at the beginning and end of the jet structure. Nakamura and Plumb (1994) examined the dependence of the direction of Rossby wave breaking on the across-jet flow symmetry. They showed that for realistic jets the rate of strain is larger equatorward of the jet and that this leads to wave breaking that transports air across the jet toward the equator (so-called equatorward wave breaking). We therefore expect there to be predominantly equatorward wave breaking in SJ sectors, with “tongues” of high-EPV air (EPV is negative in the SH, and we use “high EPV” air to mean air with a high absolute value of EPV) extending toward the equator. Whether this tongue thins and tilts upstream or broadens and rolls up cyclonically depends on the mean barotropic shear (Thorncroft et al. 1993).

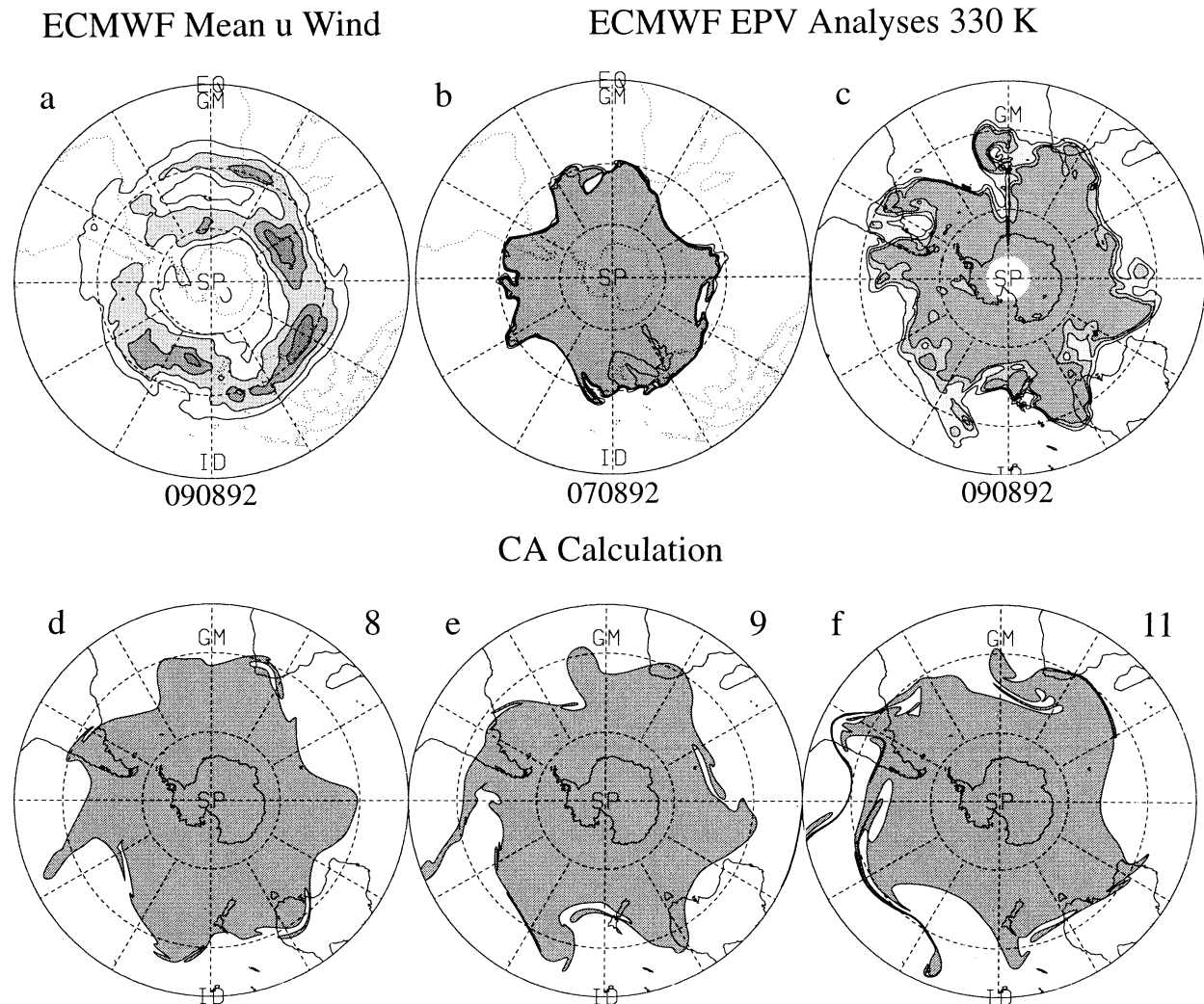


FIG. 4. Zonal wind, EPV, and CA calculations on the 330-K isentropic surface 7–11 Aug 1992. (a) Mean zonal wind over a 5-day period (contour interval and shading as in Fig. 1), (b) smoothed EPV on 7 Aug (thin contours are for -2 and -3 PVU, thick for -2.5 PVU, and values smaller than -2.5 PVU are shaded), (c) EPV on 9 Aug (thin contours are for -2 , -3 , and -4 PVU, and values smaller than -2 PVU are shaded), and (d), (e), (f) CA calculations on 8, 9, and 11 Aug (the calculation was initialized with the smoothed EPV = -2.5 PVU contour on 7 Aug). In the CA calculations the region smaller than -2.5 PVU is shaded. Maps are polar stereographic projections; the outer circle is the equator in (a), (b) and 15°S in (c), (d), (e), (f); dashed circles are 30° and 60°S .

Figure 4 shows the mean zonal wind, EPV maps, and results from a CA calculation for 7–11 August 1992, when the Australian sector is in the SJ configuration (Fig. 4a). EPV maps and CA calculations show a Rossby wave propagating eastward along this jet and then amplifying as it approaches the end of the jet (8–9 August). This leads to an equatorward wave-breaking event between 150° and 180°W around 10–11 August. The CA calculation shows that the extruded tongue tilts westward (upstream) and rolls up cyclonically. The latter developments are not seen in the PV maps because of the relatively fast diabatic decrease of EPV in the subtropics. However, maps of the EPV = -1 PVU contour for this same period (not shown) show a cyclonic air mass near 20°S , 160°W in very good agreement with

the CA calculations. During this period there is also an equatorward, cyclonic wave-breaking event over the eastern Pacific Ocean (90° – 120°W , 7–8 August), where the jet structure is also characteristic of the SJ configuration. The above evolution in both sectors is consistent with that expected from the above barotropic shear arguments and from previous examinations of the nonlinear evolution.

In the three other configurations there are significant zonal variations within the sector, and these variations can lead to different Rossby wave evolution. In the BJ configuration there is a weakening of the subtropical jet, and it is well documented, by modeling and observational studies, that wave breaking is confined within regions of weak zonal winds (e.g., Nakamura 1994; Pe-

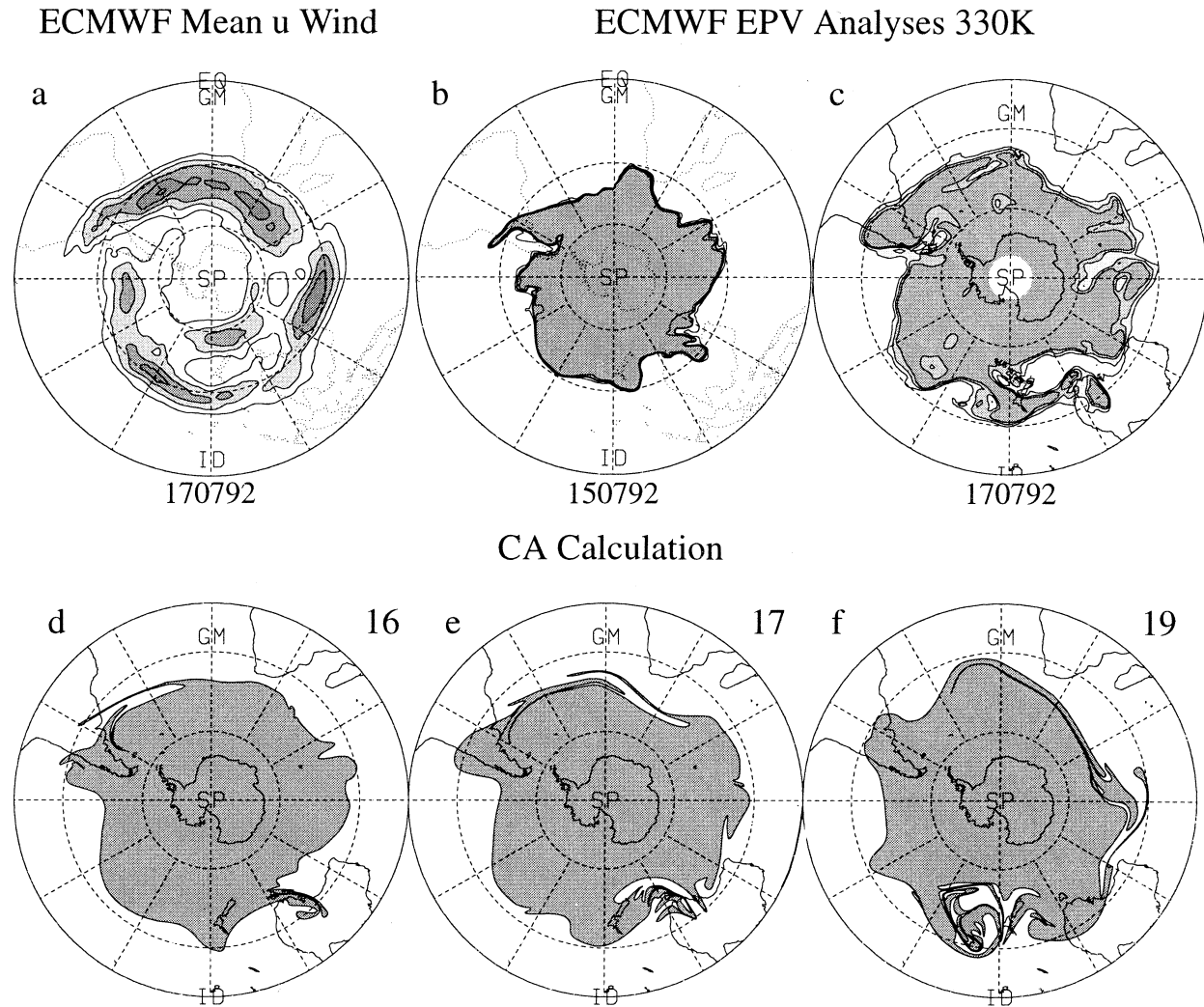


FIG. 5. As in Fig. 4, but for 15–19 Jul 1992.

ters and Waugh 1996; Swanson et al. 1997; Waugh and Polvani 2000). We therefore expect when the sector flow is in the BJ configuration for the wave breaking to occur in the region where the subtropical jet weakens. Furthermore, Nakamura (1994) and Peters and Waugh (1996) have shown that the curvature of the flow in this region is such that the wave breaking is primarily poleward (i.e., there is advection of low-EPV air toward the pole) and that the intruded air wraps up in anticyclonic motion. Nevertheless, for specific wind configurations with locally weakened backstream wind equatorward wave breaking is also possible, as was shown by Swanson (2000). In some BJ cases there is a strong polar jet in the gap in the subtropical jet (see previous section), and the anticyclonic shear supports the anticyclonic roll-up of air advected poleward in the wave breaking.

Figure 5 shows the same quantities as Fig. 4 but for 15–19 July 1992. During this period the basic flow in the Australian sector is in the BJ configuration; that is,

the subtropical jet weakens over southern Australia. EPV and CA maps show a Rossby wave propagating eastward over southern Australia, which strongly amplifies around 16 July, and then breaks poleward within the region of weak zonal winds on 17 July. The low-EPV air advected poleward in the event rolls up anticyclonically over New Zealand on 19 July and, according to the CA calculation, “re-merges” with the subtropical jet. Note that in this case there are some differences between the EPV and CA calculations. The EPV maps show a large region of low EPV being entrained and forming an isolated region of low EPV poleward of the jet, whereas the CA calculation shows only a thin tongue of low EPV that wraps up anticyclonically. One reason for this difference is that there is a preexisting region of low EPV poleward of the subtropical jet that is not included in the CA calculations, and the merging of this air and the newly entrained low-EPV air is captured in the EPV but not in the CA calculations.

Note that similar behavior and differences between EPV and CA calculations can be seen in the wave breaking over the Northern Pacific in Figs. 3 and 4 of Peters and Waugh (1996).

The expected behavior in the DD configuration is similar to that in the BJ configuration. The anticyclonic flow due to the polar jet will likely dominate the flow at the end of the subtropical jet, and as the Rossby wave propagates in decreasing winds at the end of the subtropical jet we expect poleward wave breaking with anticyclonic behavior (i.e., the low-EPV air rolls up into an anticyclone). Figure 6 shows the same quantities as Fig. 4 but for the period 8–12 June 1990, during which the basic flow over the central Pacific region is in a DD configuration; that is, the polar jet is lying downstream of the subtropical maximum over the Pacific Ocean. During this period there are two intrusions of air masses with low EPV into polar latitudes (see 10 June maps): one over the central Pacific Ocean in which there is a DD background wind configuration and the other over the region to the west of New Zealand where a more BJ wind structure exists. The upstream-intruding air over the central Pacific was produced by a poleward-breaking Rossby wave, and the strong influence of the anticyclonic shear of the polar jet results in the anticyclonic rollup of this air. The air mass remains stationary for 3–5 days (i.e., a blocking high) before it moves northeastward and is stretched by the subtropical jet (12–13 June). The downstream-intruded air mass near New Zealand follows a similar evolution. The tip of the tongue of low EPV rolls up anticyclonically and then drifts slowly eastward under the influence of the stronger anticyclonic shear of the polar jet. It enters the same region of the first-event remains, caused by the same DD background zonal-wind configuration. The air mass over the central Pacific Ocean that moves equatorward (11 June) is slightly wrapped up cyclonically by the strong cyclonic shear of the subtropical jet (12–13 June).

In the DU configuration, waves propagating along the polar jet will be influenced by both the polar jet and subtropical jet, and the expected behavior will depend on the relative strengths of the jets. If the jets are of roughly comparable strength (i.e., there is symmetry between the anticyclonic wind shear of the polar jet and the cyclonic shear of the subtropical jet), air may be advected poleward but tilts downstream rather than rolling up (as in the DD configuration).

A period when the Australian sector is in a DU configuration (1–5 June 1993) is shown in Fig. 7. Around 3 June a poleward Rossby wave breaking occurs southwest of Australia. The symmetry between the anticyclonic wind shear of the polar jet and the cyclonic shear of the subtropical jet means that the low-EPV air advected to the south does not roll up but rather tilts downstream. So this wave breaking is better described as “symmetric” breaking than as poleward or equatorward. A second wave-breaking event, with the same

general characteristics, begins in roughly the same region at the end of the period shown. The initial stages of this event can be seen over the Indian Ocean in the 5 June maps. Further examples of wave breaking in regions with DU configuration can be seen over the South Atlantic in Fig. 4 (8–9 August 1992) and over the eastern Pacific in Fig. 5 (16–17 July 1992). The flow evolution in these regions is similar to the event in the Australian sector shown in Fig. 7.

It is important to note that the specific evolution depends on the amplitude of Rossby waves, the strength of the jet(s), and the horizontal shear. So the preceding should be considered general statements for relatively similar conditions and not necessarily rules that always apply, as discussed by Peters and Waugh (1996).

b. General remarks

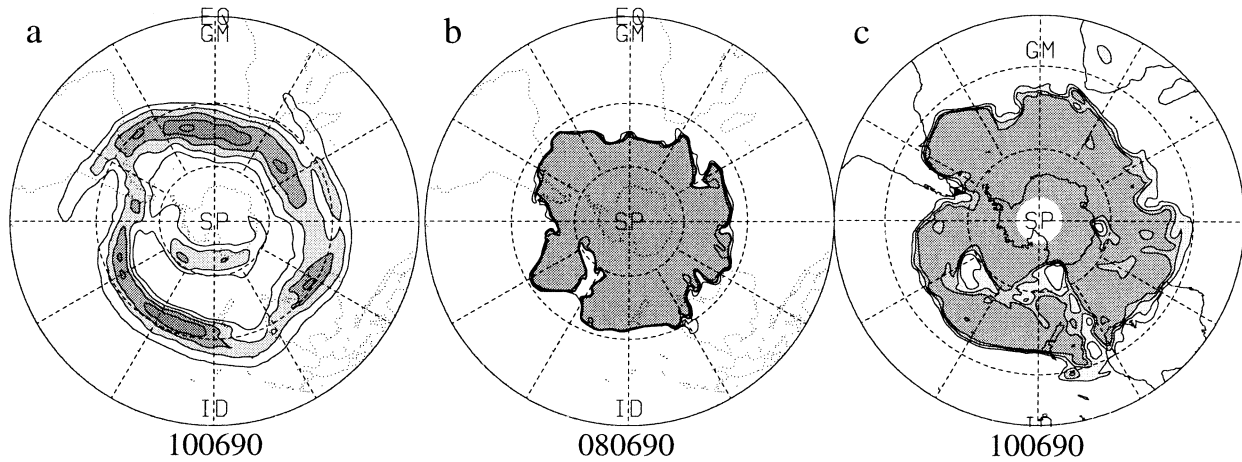
The four case studies discussed previously show that, consistent with simple barotropic shear arguments, the Rossby wave propagation and breaking differs when the flow in the Australia–central Pacific region is different. We have performed CA calculations and examined PV maps for the four winters from 1990 to 1993, and there is a good correspondence between the configuration in a sector and the characteristics of the Rossby wave breaking.

The flow structure within all sectors varies on a wide range of timescales, and the submonthly variability is generally larger than the month-to-month variability. On submonthly timescales all four configurations occur in all sectors. However, the frequency and characteristics are different. The latitudes of the jet when the Atlantic and Indian Ocean sectors are in the SJ configuration are variable, and in these sectors the jet appears as a subtropical or polar jet. In the other sectors the latitude of the SJ does not vary as much, but there is variability in the longitudinal extent, and an extended subtropical jet covering both the Australian and Pacific Ocean sectors can occur. The BJ configuration, with two relatively separated wind maxima in one sector, also occurs in every sector, but most often in the Australian and Pacific Ocean sectors. Only in these sectors is a secondary zonal-wind maximum, poleward of the gap between both the subtropical maxima, observed to occur. Although on submonthly timescales double jets occur in all sectors, the DU configuration occurred most often in the Australian sector, and the DD configuration was most often in the Pacific Ocean sector.

Because of these differences in preferred zonal-wind configurations there are differences in the wave breaking in each geographical sector. The background zonal wind is highly variable in the Australian and Pacific Ocean sectors, and CA calculations and EPV maps show high variability in the characteristics of the wave breaking in these sectors. As the Atlantic and Indian Ocean sectors are almost always in an SJ configuration, wave breaking in these sectors is almost always equa-

ECMWF Mean u Wind

ECMWF EPV Analyses 330K



CA Calculation

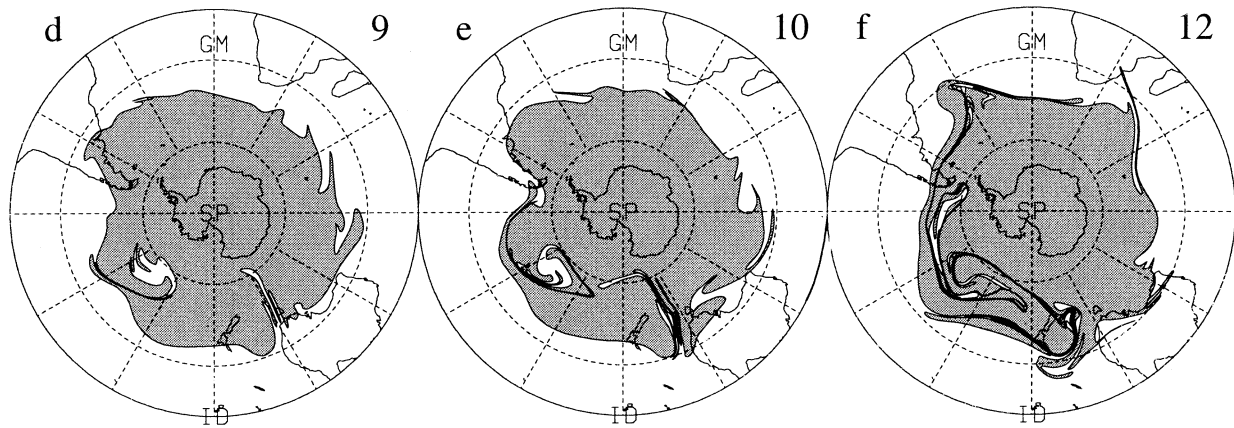


FIG. 6. As in Fig. 4, but for 8–12 Jun 1990.

toward. Equatorward breaking is also common over the eastern Pacific Ocean. Poleward breaking occurs when there is a BJ, DU, or DD configuration in one sector, and, as a consequence of the above preferred regions for broken and double jets, there are two main centers for poleward breaking: one over the eastern Indian Ocean–New Zealand region and the other over the Pacific Ocean. Which region the poleward breaking occurs in varies between months and years.

5. Discussion

Consideration of these idealized flow configurations provides insight into the characteristics of Rossby wave propagation and breaking in the SH upper troposphere, which may impact other phenomena. For example, the fact that poleward breaking has two main centers—one over the eastern Indian Ocean–New Zealand region and

the other over the Pacific Ocean—has several possible consequences.

Several studies have shown that the same two regions are the primary regions for blocking in the SH (e.g., Kiladis and Mo 1998; Mo and Higgins 1998; Sinclair 1996). The poleward-breaking events entrain low-EPV air that rolls up anticyclonically, often producing a cut-off region of low EPV. Furthermore, these events are observed to occur in series, with the newly entrained low-EPV air from one event merging with similar air from previous events. Such a sequence contributes to the formation and maintenance of blocks. Analysis of the winters from 1990 to 1993 shows interannual and intraseasonal variations in the locations of the poleward breaking (see section 4b), and it would be interesting to see if decadal variations are observed in blocking events.

The preferred regions for poleward-breaking events

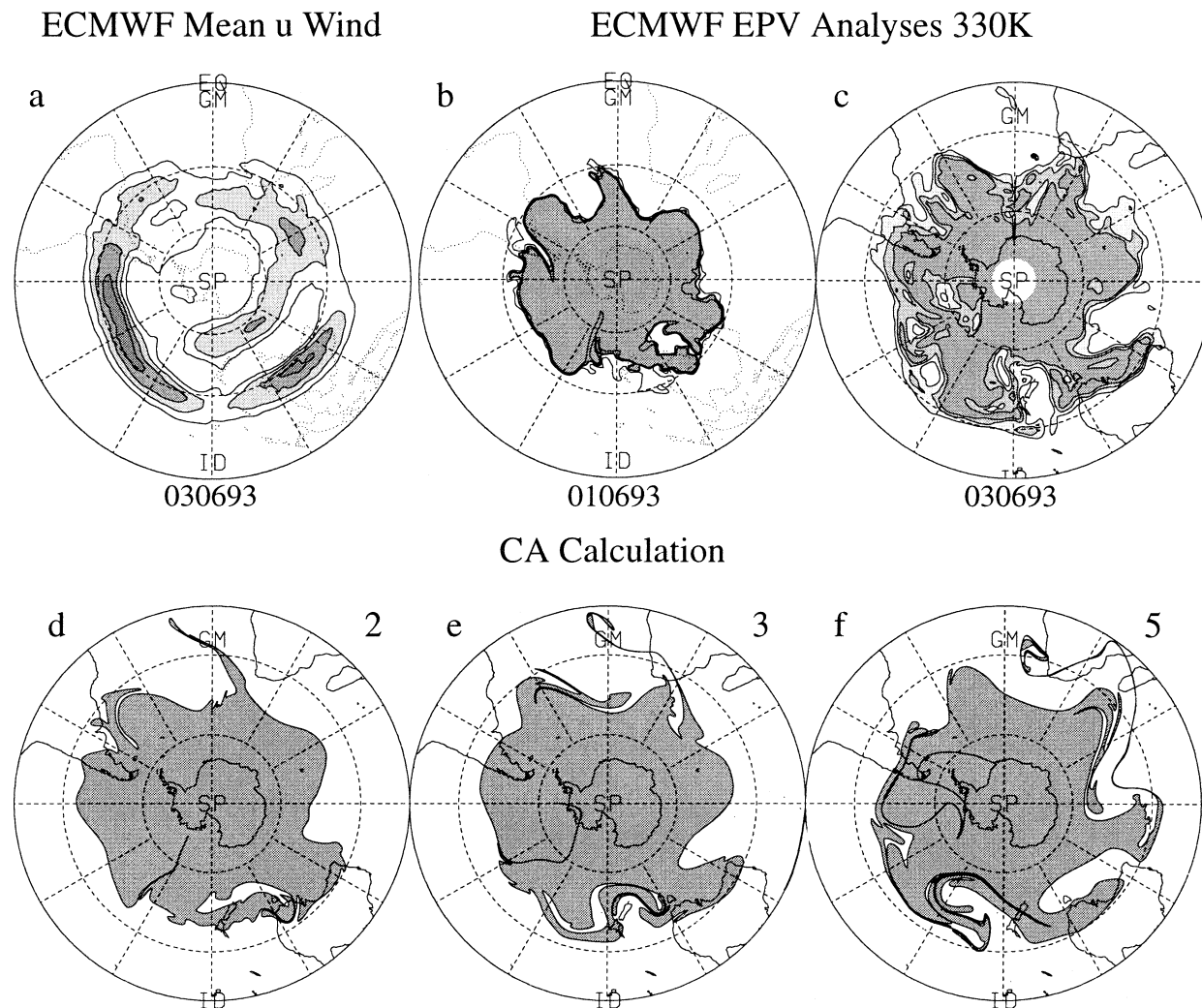


FIG. 7. As in Fig. 4, but for 1–5 Jun 1993.

may also impact the distribution of total ozone, and in particular the occurrence of “ozone miniholes” [synoptic-scale decreases in total ozone that are separate from the planetary-scale ozone hole that forms over Antarctica in spring (e.g., Newman et al. 1988; McKenna et al. 1989)]. Ozone miniholes occur in both the Southern and Northern Hemispheres (Entzian et al. 1992; McCormack and Hood 1997; James 1998a,b; Vignarolo et al. 2001). It is well known, since the work of Dobson et al. (1929), that synoptic-scale decreases (increases) in total ozone are linked with anticyclones (cyclones) in midlatitudes, and several recent studies have shown that poleward Rossby-wave-breaking events play a key role in the formation of ozone miniholes in the Northern Hemisphere (e.g., Peters et al. 1995; James et al. 2000; James and Peters 2002). We therefore expect an increased number of minihole events in the preferred regions of (anticyclonic) poleward wave breaking. This is confirmed by the analysis of James (1998a), which shows the highest number of “mini-hole days” for ex-

tended austral winters in the Australian sector. Again, it would be interesting to examine intraseasonal, interannual, and decadal variations in the occurrence of these events.

A further consequence of the poleward-breaking events may be the generation of inertia–gravity waves near the tropopause that propagate upstream with downward energy propagation in the troposphere and upward energy propagation in the stratosphere. Localized regions of strong winds at the tropopause, “jet streaks,” are known to excite inertia–gravity waves by ageostrophic adjustment or shear instability (e.g., O’Sullivan and Dunkerton 1995). These jet streaks occur southeast of poleward-breaking events, and, hence, these breaking events may excite inertia–gravity waves. One such case is discussed by Guest et al. (2000, their Fig. 15), where observed inertia–gravity waves are linked to a strong polar jet streak connected with two poleward-wave-breaking events, one related to a DU wind structure over the eastern Indian Ocean and one related to a BJ struc-

ture over Tasmania. Further study is needed to confirm any link between particular types of Rossby wave breaking and excitation of inertia-gravity waves.

6. Summary

Analysis of the wintertime upper-tropospheric flow in the Southern Hemisphere shows that there are significant zonal variations. The flow in different sectors ($\approx 120^\circ$ longitude) can differ, and there can be significant longitudinal variations within a sector. Furthermore, there is both intraseasonal and interannual variability in the flow in a given geographical sector. We identify four typical flow configurations for flow in a sector: a single jet (SJ), a broken subtropical jet (BJ), a polar jet at the upstream end of the subtropical jet (DU), and a polar jet at the downstream end of the subtropical jet (DD). We further argue, on the basis of barotropic shear arguments, that the characteristics of Rossby wave breaking will be different for the different basic-state configurations, and that there is equatorward wave breaking with cyclonic behavior when in an SJ configuration, poleward breaking with anticyclonic behavior when in a BJ or DD configuration, and more symmetric wave breaking when in a DU configuration. Four case studies, when there was a different flow configuration in the Australia-central Pacific region, are presented that support these simple shear arguments.

Visual inspection shows that some of the flow configurations have preferred geographical locations, and this results in different geographical sectors having differing preferred configurations and variability and, hence, characteristics of the Rossby wave propagation. For example, a broken subtropical jet or polar jet with poleward wave breaking is most common over the eastern Indian Ocean–New Zealand and Pacific Ocean regions. As discussed in the previous section, the preference of poleward breaking to these two regions may have several consequences, including the occurrence of blocking events, ozone miniholes, and the generation of inertia-gravity waves near the tropopause; more analysis of these possible links is required.

Another future task is to examine whether idealized EPV structures consistent with the four idealized flow configurations (Fig. 3) could be used in PV-evolution calculations (e.g., contour dynamics), where the evolving wind was a function of PV evolution. This would clarify the relative role of diabatic and baroclinic processes in determining the evolution during the wave-breaking events.

Acknowledgments. This project was carried out within the Deutsches Ozonforschungsprogramm des Bundesministerium fuer Bildung, Wissenschaft, Forschung und Technologie (Grant 01 LO 9510/5), as D. P. was visiting the Cooperative Research Center for Southern Hemisphere Meteorology at Monash University in Melbourne, Australia. The authors thank David Karoly for

his support of this work, William Randel for providing the NCEP–NCAR reanalysis data, and the Deutscher Wetterdienst and Deutsches Klimarechenzentrum for making available ECMWF analysis data.

REFERENCES

- Appenzeller, C., H. C. Davies, and W. A. Norton, 1996: Fragmentation of stratospheric intrusions. *J. Geophys. Res.*, **101**, 1435–1456.
- Bals-Elsholz, T. M., E. H. Atallah, L. F. Bosart, T. A. Wasula, M. J. Cempa, and A. R. Lupo, 2001: The wintertime Southern Hemisphere split jet: Structure, variability, and evolution. *J. Climate*, **14**, 4191–4215.
- Bartels, J., D. Peters, and G. Schmitz, 1998: Climatological Ertel's potential vorticity flux and mean meridional circulation in the extratropical troposphere–lower stratosphere. *Ann. Geophys.*, **16**, 250–265.
- Chen, B. S., R. Smith, and D. H. Bromwich, 1996: Evolution of the tropospheric split jet over the South Pacific Ocean during the 1986–1989 ENSO cycle. *Mon. Wea. Rev.*, **124**, 1711–1731.
- Dobson, G. M. B., D. N. Harrison, and J. Lawrence, 1929: Measurements of the amount of ozone in the earth's atmosphere and its relation to other geophysical conditions: Part III. *Proc. Roy. Soc. London*, **A122**, 456–486.
- Entzian, G., D. Peters, K. Grasnick, U. Feister, K. Wege, and U. Koehler, 1992: Eigenschaften von Ozone Mini-Holes mittlerer Breiten. *Ann. Meteor.*, **27**, 196.
- Ertel, H., 1942: Ein neuer hydrodynamischer Wirbelsatz. *Meteor. Z.*, **59**, 277–281.
- Guest, F. M., M. J. Reeder, C. J. Marks, and D. J. Karoly, 2000: Inertia-gravity waves observed in the lower stratosphere over Macquarie Island. *J. Atmos. Sci.*, **57**, 737–752.
- Hartmann, D. L., 1995: A PV view of zonal flow vacillation. *J. Atmos. Sci.*, **52**, 2561–2576.
- Hoskins, B. J., I. N. James, and G. H. White, 1983: The shape, propagation and mean-flow interaction of large-scale weather systems. *J. Atmos. Sci.*, **40**, 1595–1612.
- , M. E. McIntyre, and A. W. Robertson, 1985: On the use and significance of isentropic potential vorticity maps. *Quart. J. Roy. Meteor. Soc.*, **111**, 877–946.
- , and —, 1987: Reply. *Quart. J. Roy. Meteor. Soc.*, **113**, 402–404.
- , H. H. Hsu, I. N. James, M. Masutani, P. D. Sardeshmukh, and G. H. White, 1989: Diagnostics of the global atmospheric circulation. WCRP Rep. 27, WMO Tech. Doc. 326, 217 pp.
- James, P. M., 1998a: An interhemispheric comparison of ozone mini-hole climatologies. *Geophys. Res. Lett.*, **25**, 301–304.
- , 1998b: A climatology of ozone mini-holes over the Northern Hemisphere. *Int. J. Climatol.*, **18**, 1287–1303.
- , and D. Peters, 2002: The Lagrangian structure of ozone mini-holes and potential vorticity anomalies in the Northern Hemisphere. *Ann. Geophys.*, **20**, 836–846.
- , and D. W. Waugh, 2000: Very low ozone episodes due to polar vortex displacement. *Tellus*, **52B**, 1123–1137.
- Kalnay, E., and Coauthors, 1996: The NCEP/NCAR 40-Year Reanalysis Project. *Bull. Amer. Meteor. Soc.*, **77**, 437–471.
- Karoly, D. J., 1989: Southern Hemisphere circulation features associated with El Niño–Southern Oscillation events. *J. Climate*, **2**, 1239–1252.
- , 1990: The role of transient eddies in low-frequency zonal variations of the Southern Hemisphere circulation. *Tellus*, **42A**, 41–50.
- Kidson, J. W., 1988: Indices of Southern Hemisphere zonal wind. *J. Climate*, **1**, 183–194.
- Kiladis, G. N., and K. C. Mo, 1998: Interannual and intraseasonal variability in the Southern Hemisphere. *Meteorology of the Southern Hemisphere*, Meteor. Monogr., No. 49, Amer. Meteor. Soc., 307–336.
- McCormack, J. P., and L. L. Hood, 1997: The frequency and size of

- ozone "mini-hole" events at northern midlatitudes in February. *Geophys. Res. Lett.*, **24**, 2647–2650.
- McIntyre, M. E., and T. N. Palmer, 1983: Breaking planetary waves in the stratosphere. *Nature*, **305**, 593–600.
- McKenna, D. S., R. L. Jones, J. Austin, E. V. Browell, M. P. McCormick, A. J. Krueger, and A. F. Tuck, 1989: Diagnostic studies of Antarctic vortex during the 1987 airborne Antarctic ozone experiment: Ozone miniholes. *J. Geophys. Res.*, **94**, 11 641–11 668.
- Mo, K. C., and R. W. Higgins, 1998: The Pacific–South American modes and tropical convection during the Southern Hemisphere winter. *Mon. Wea. Rev.*, **126**, 1581–1596.
- Nakamura, M., 1994: Characteristics of potential vorticity mixing by breaking Rossby waves in the vicinity of a jet. Sc.D. thesis, Massachusetts Institute of Technology, 253 pp.
- , and R. A. Plumb, 1994: The effects of flow asymmetry on the direction of Rossby wave breaking. *J. Atmos. Sci.*, **51**, 2031–2045.
- Newman, P. A., L. R. Lait, and M. R. Schoeberl, 1988: The morphology and meteorology of Southern Hemisphere spring total ozone mini-holes. *Geophys. Res. Lett.*, **15**, 923–926.
- Nigam, S., 1990: On the structure of variability of the observed tropospheric and stratospheric zonal-mean zonal winds. *J. Atmos. Sci.*, **47**, 1799–1813.
- Norton, W. A., 1994: Breaking Rossby waves in a model stratosphere diagnosed by a vortex-following coordinate system and a technique for advecting material contours. *J. Atmos. Sci.*, **51**, 654–673.
- O’Sullivan, D., and T. J. Dunkerton, 1995: Generation of inertia-gravity waves in a simulated life cycle of baroclinic instability. *J. Atmos. Sci.*, **52**, 3695–3716.
- Peters, D., and D. W. Waugh, 1996: Influence of barotropic shear on the poleward advection of upper tropospheric air. *J. Atmos. Sci.*, **53**, 3013–3031.
- , J. Egger, and G. Entzian, 1995: Dynamical aspects of ozone mini-hole formation. *Meteor. Atmos. Phys.*, **5**, 205–214.
- Plumb, R. A., and Coauthors, 1994: Intrusions into the lower stratospheric Arctic vortex during the winter of 1991/92. *J. Geophys. Res.*, **99**, 1089–1106.
- Randel, W. J., 1992: Global atmospheric circulation statistics 1000–1 mb. NCAR Tech. Note NCAR/TN-366+STR, 256 pp.
- Sinclair, M. R., 1996: A climatology of anticyclones and blocking for Southern Hemisphere. *Mon. Wea. Rev.*, **124**, 245–263.
- Swanson, K. L., 2000: Stationary wave accumulation and the generation of low-frequency variability on zonally varying flows. *J. Atmos. Sci.*, **57**, 2262–2280.
- , J. Kushner, and I. M. Held, 1997: Dynamics of barotropic storm tracks. *J. Atmos. Sci.*, **54**, 791–810.
- Thorncroft, C. D., B. J. Hoskins, and M. E. McIntyre, 1993: Two paradigms of baroclinic-wave life-cycle behavior. *Quart. J. Roy. Meteor. Soc.*, **119**, 17–55.
- Trenberth, K. E., 1991: Storm tracks in the Southern Hemisphere. *J. Atmos. Sci.*, **48**, 2159–2178.
- Vigliarolo, P. K., C. S. Vera, and S. B. Diaz, 2001: Southern Hemisphere winter ozone fluctuations. *Quart. J. Roy. Meteor. Soc.*, **127**, 559–577.
- Waugh, D. W., and R. A. Plumb, 1994: Contour advection with surgery: A technique for investigating fine scale structure in tracer transport. *J. Atmos. Sci.*, **51**, 530–540.
- , and L. M. Polvani, 2000: Intrusions into the tropical upper troposphere. *Geophys. Res. Lett.*, **27**, 3857–3860.
- , and Coauthors, 1994: Transport of material out of the stratospheric Arctic vortex by Rossby wave breaking. *J. Geophys. Res.*, **99**, 1071–1088.